Journal of Nuclear Materials 386–388 (2009) 634–638

Contents lists available at ScienceDirect

Journal of Nuclear Materials

journal homepage: www.elsevier.com/locate/jnucmat

Microstructural optimization of high-temperature SiC/SiC composites by NITE process

K. Shimoda [a,*], J.S. Park [b], T. Hinoki [a], A. Kohyama [a]

[a] *Institute of Advanced Energy, Kyoto University, Gokasho, Uji, Kyoto 611-0011, Japan*
[b] *Institute of Energy Science and Technology Co., Ltd., Toshima-ku, Tokyo 171-0021, Japan*

ABSTRACT

Two kinds of SiC fiber-reinforced SiC (SiC/SiC) composites (high strength type and high ductility type) were prepared by NITE process and their thermo-mechanical properties were investigated from room to high temperature. Furthermore, thermal stress figure of merit of advanced SiC/SiC composites including prepared NITE-SiC/SiC composites were discussed. Matrix densification, especially inter-fiber-tows, was effective way to restrict the oxygen diffusion through pores and hence fiber and matrix interface was protective against the oxidation. In NITE process, excess additional additives for matrix densification, like high ductility type, caused weight loss with pore formation derived from the oxide segregations over 1300 °C. There was no degradation in strength by 1500 °C and simultaneously high thermal conductivity was kept up to 1500 °C for high strength type, resulting in the excellent thermal figure of merit.

1. Introduction

Continuous silicon carbide fiber-reinforced silicon carbide (SiC/SiC) composites are one of the promising structural materials for future fusion reactors because of the excellent potentiality in thermal and mechanical properties under very severe environment including high temperature and high energy neutron bombardment [1–3]. For fusion-grade SiC/SiC composites, high-crystallinity and near-stoichiometric characteristics are required to keep excellent stability against neutron irradiation [4]. The realization of fusion reactors will be strongly depend on optimization of SiC/SiC composites microstructure, particularly in regard to the materials and processes used for the fiber, interface and matrix constituents [1,2,5]. One of the important accomplishments is a new process, called nano-infiltration and transient eutectic phase (NITE) process developed in our group at Kyoto University [6–8]. The microstructure in NITE-SiC/SiC composites, such as fiber volume fraction, porosity and type of pores, can be controlled precisely by the tailoring raw materials and the selection of fabrication temperature/applied stress history. For instance, two kinds of attractive highly-dense SiC/SiC composites in fracture behavior (high strength type and high ductility type) were successfully fabricated by NITE process [9]. The objective of this study is to investigate thermal stability and thermo-mechanical properties of advanced SiC/SiC composites including these two kinds of NIT SiC/SiC composites at high temperature.

2. Experimental procedure

Tyranno-SA fiber grade-3 SiC fiber (Ube Industries. Ltd., Ube, Japan) was employed as reinforcements in unidirectional (UD) and 0/90° cross-plied (CP) architecture. Pyrolytic carbon (PyC) interface was deposited on the fiber surface through chemical vapor deposition (CVD) process. Two kinds of attractive highly-dense SiC/SiC composites in fracture behavior (high strength type and high ductility type) were prepared with NITE process in our laboratory. Details of the fabrication procedure are described elsewhere [9]. Table 1 lists fabrication conditions and typical properties. The straight bar type specimens were prepared for the exposure tests. The specimens are $1.5^{W}*40^{L}*3^{T}$ mm^3 in dimension. Specimens were placed in a carbon crucible and then exposed from 1000 °C to 1500 °C for 1 h in Ar–O_2 gas mixture with an oxygen partial pressure of $PO_2 = 0.1$ Pa (10^{-7} atm). The furnace containing specimens was cooled by room-temperature. Specimens were carefully weighted before and after the exposure test to obtain weight change by an electronic balance. Microstructural evolution after exposure was observed by field emission scanning electron microscopy (FE-SEM). Mechanical properties were evaluated by monotonic tensile test using an Instron 5581 load frame following the general guidelines of ASTM C1275. On both edges of the tensile bars, the aluminum tabs were affixed to each side using a kind of standard Araldite binder. The gauge length was designated to be 20 mm. Tensile strain was recorded from the extensometer fixed on both

---

* Corresponding author. Address: Graduate School of Energy Science, Kyoto University, Gokasho, Uji, Kyoto 611-0011, Japan. Tel.: +81 774 38 3465; fax: +81 774 38 3467.

E-mail address: k-simd@iae.kyoto-u.ac.jp (K. Shimoda).

0022-3115/$ - see front matter © 2008 Elsevier B.V. All rights reserved.
doi:10.1016/j.jnucmat.2008.12.234

Table 1
Fabrication conditions and typical properties of two kinds of NITE-SiC/SiC composites.

Material	High strength type		High ductility type	
Architecture	UD	CP	UD	CP
Reinforcement	Tyranno™-SA grade-3			
Fiber-matrix I/F	PyC$^{0.5\ \mu m}$			
Matrix	SiC + 12wt%addtives		SiC + 18wt%addtives	
Fabrication temperature	1900 °C		1800 °C	
Fiber volume fraction	53 vol.%	51 vol.%	52 vol.%	53 vol.%
Density	3.11 Mg/m^3	3.06 Mg/m^3	2.98 Mg/m^3	2.96 Mg/m^3
Relative density	99%	96%	95%	94%
Porosity	0.6%	3.8%	1.6%	1.2%
Tensile properties				
Proportional limit stress	*358 MPa*	*148 MPa*	209 MPa	73 MPa
Ultimate tensile strength	*408 MPa*	*167 MPa*	356 MPa	140 MPa
Strain at fracture	0.13%	0.08%	*0.22%*	*0.12%*
Elastic modulus	*358 GPa*	*288 GPa*	300 GPa	230 GPa
Thermal properties				
Thermal conductivity	32 W/m K		21 W/m K	

sides of the gauge areas. Thermal diffusivities were measured in a through-thickness direction for UD samples (nominally 10 mm diameter and 2 mm in thickness) at the temperature range from room temperature to 1500 °C in Ar using laser flash equipment. Thermal diffusivity (α) was obtained by $t_{1/2}$ method. Thermal conductivity (K_{th}) was calculated by $\alpha * C_p * \rho$, where C_p and ρ are specific heat and bulk density, respectively. Specific heat was measured by laser flash principle below 600 °C and by thermo-penetration principle over 600 °C. The thermal stress figure of merit (M) was calculated by $\sigma_{PLS} * K_{th} * (1 - \nu)/(\alpha_{th} * E)$, where σ_{PLS}, ν, α_{th} and E are proportional limit stress (PLS), Poisson's ratio, coefficient of thermal expiation and elastic modulus, respectively.

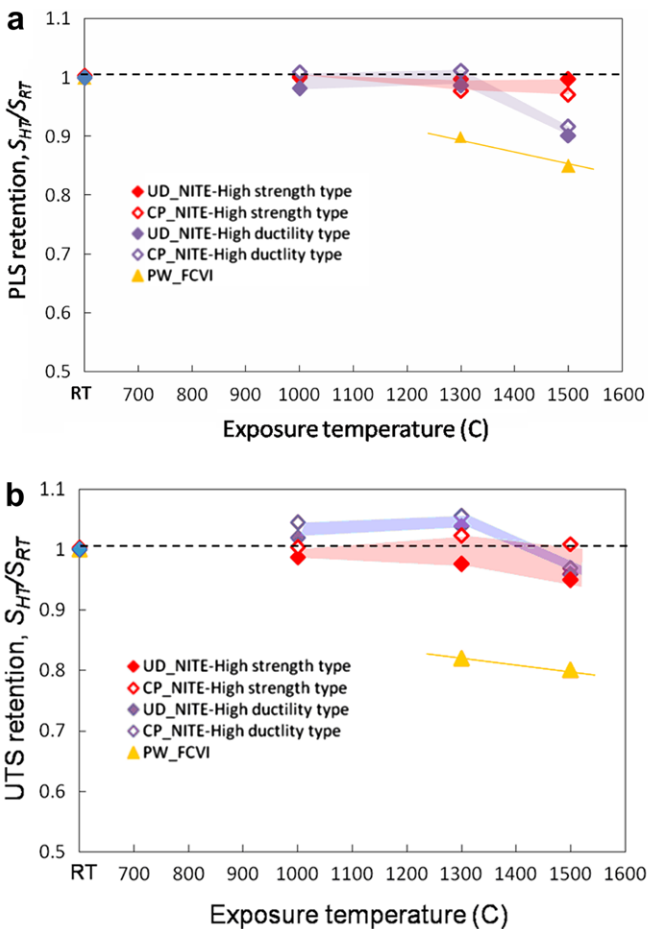

Fig. 1. Monotonic tensile test results of FCVI- and two kinds of NITE-SiC/SiC composites after exposure: (a) proportional limit stress (PLS) retention and (b) ultimate tensile stress (UTS) retention.

3. Results

3.1. Mechanical properties at high-temperature

Fig. 1(a) and (b) show proportional limit stress (PLS) and ultimate tensile strength (UTS) retentions of plain woven (PW) FCVI- and two kinds of NITE-SiC/SiC composites after exposure. About 10% degradation in PLS and about 20% degradation in UTS after exposure of 1300 °C for FCVI-SiC/SiC composites. However, two kinds of NITE-SiC/SiC composites showed the excellent PLS and UTS retentions after exposure of 1300 °C in spite of fiber architecture. In addition, there was no degradation by exposure of 1500 °C for high strength composites. PLS of high ductility type was decreased by about 10% after 1500 °C. Fig. 2 shows the fracture behavior of two kinds of NITE-SiC/SiC composites after exposure ((a) high strength type and (b) high ductility type). High strength type kept non-brittle fracture behavior with both high PLS and high elastic modulus by exposure of 1500 °C. High ductility type showed non-brittle fracture behavior with a relatively long pseudo-ductile range, even though PLS and elastic modulus were slightly decreased at exposure of 1500 °C.

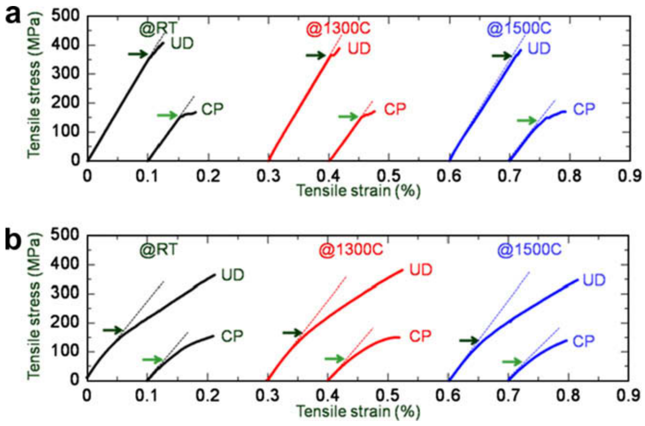

Fig. 2. Fracture behavior before and after exposure: (a) high strength type and (b) high ductility type.

3.2. Thermal stability

Fig. 3 shows backscattered electron images (BEI) taken on the polished cross-section before and after exposure at 1300 °C and 1500 °C for two kinds of NITE-SiC/SiC composites. The phases with bright contrast represent the segregations of oxide processing additives with relatively high atomic number elemental compositions. The oxide phases heavily appeared agglomerated within the SiC matrix inter-fiber-tows region for high ductility composites, while they were little detected for high strength type. The oxide phases are believed to be mostly $Y_3Al_5O_{12}$ (YAG) from XRD analysis [7,10]. The processing additives in high ductility type were increased for highly-dense matrix with the workability of SiC nano-powder, resulting in SiC matrix formation with a lot of oxide segregations. Most of the SiC/SiC composites, even for the CVI-SiC/SiC composites with high-purity matrix, underwent the reduction in both UTS and PLS by about ~20% at 1300 °C. In particular, this reduction was attributed to a slight burnout of the carbon interface due to oxygen impurities in test atmosphere, as shown in Fig. 4. However, there was no significant degradation for high ductility type by 1300 °C and for high strength type by 1500 °C. CVI-SiC/SiC composites usually contains 10–20% porosity, mainly inter-fiber-tows. Highly-dense matrix by NITE process, especially inter-fiber-tows, could restrict the oxygen diffusion through pores and hence fiber and matrix interface was protective against the oxidation. About 12% degradation in PLS for only high ductility type at 1500 °C is supposed because the composites exhibited a marked mass loss (about 3%) by the active oxidation of the SiC grains occurred concurrently with the vaporization of the oxide segregations which was comprised mainly of the additional additives, as

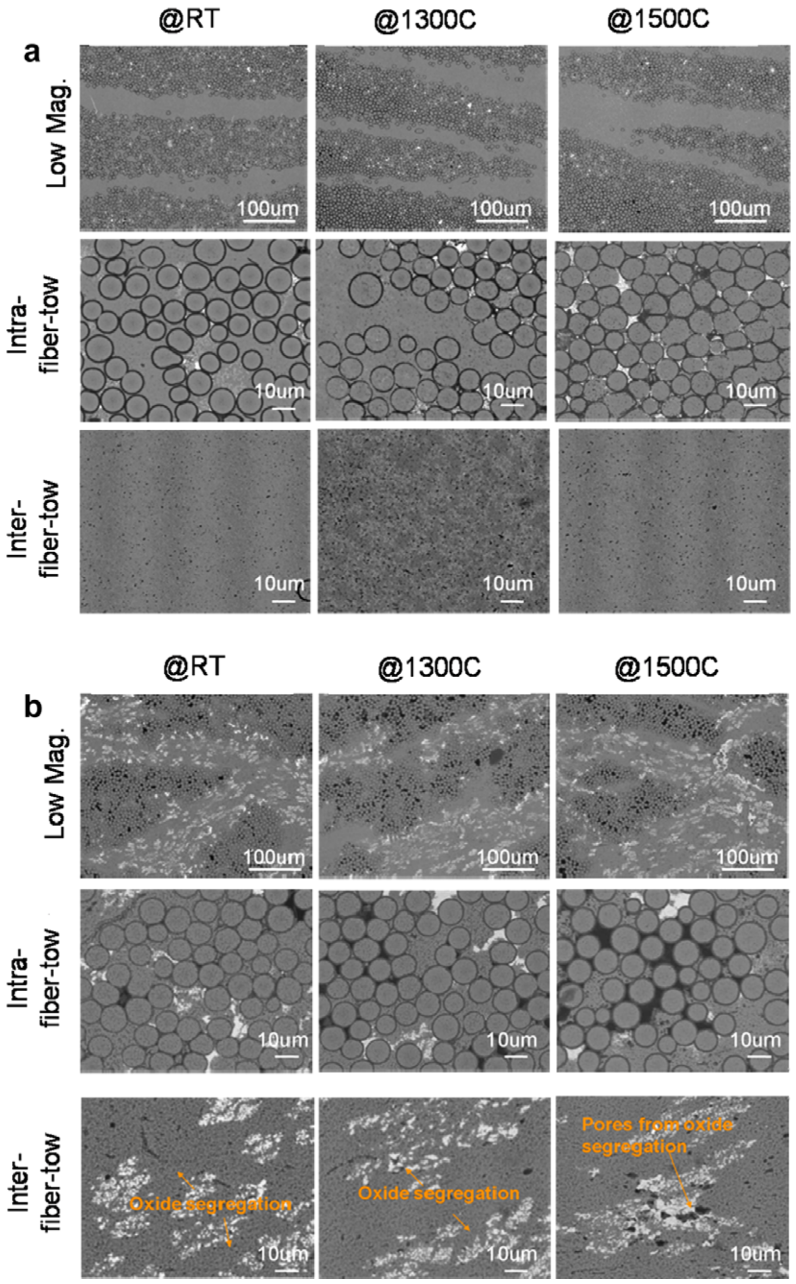

Fig. 3. Backscattered electron images (BEI) taken on the polished-section before and after exposure at 1300 °C and 1500 °C: (a) UD_high strength type and (b) UD_high ductility type.

shown in Fig. 3(b). For high strength type, as small as possible additional additives to densify matrix could enhance the strength retention with the stability in microstructure, as the same as monolithic-SiC described elsewhere [11].

3.3. Thermal properties

Thermal conductivity of CVI- and two kinds of NITE-SiC/SiC composites measured at room and high temperature up to 1500 °C is shown in Fig. 5. Thermal conductivity of CVI-, NITE-high strength and NITE-high ductility type at room-temperature was almost 15, 21 and 32 W/m K, respectively. The thermal conductivity of high strength type was higher than that of high ductility type up to 1500 °C in spite of both highly-densified matrix formations and almost same fiber volume fraction. This might be due to SiC grain size in matrix and oxide remnants including grain boundary phase. The grain size of high ductility type was much finer (~100 nm) than that of high strength type (~300 nm) due to the difference of fabrication temperature. The grain boundary phase is considered to reduce the thermal conductivity of materials. However, the thermal conductivity of two kinds of NITE-SiC/SiC composites were much higher than that of CVI-SiC/SiC composites. This is because the pore volume fraction of NITE-SiC/SiC composites, especially inter-fiber-tows, was much smaller than that of CVI-SiC/SiC composites. The thermal conductivity of two kinds of NITE-SiC/SiC composites in this study sufficiently had satisfied completely the assumed design value for fusion reactors, whose over 15 W/m K is required at 1000 °C [12,13].

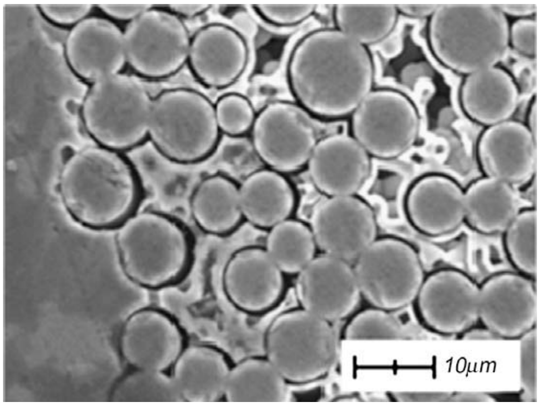

Fig. 4. Secondary electron image (SEI) taken on the polished-section of CVI-SiC/SiC composites after exposure of 1300 °C.

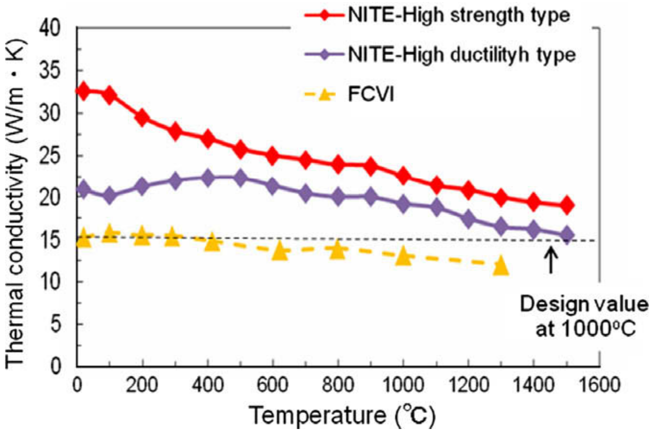

Fig. 5. Thermal conductivity of CVI- and two kinds of NITE-SiC/SiC composites from room-temperature to 1500 °C.

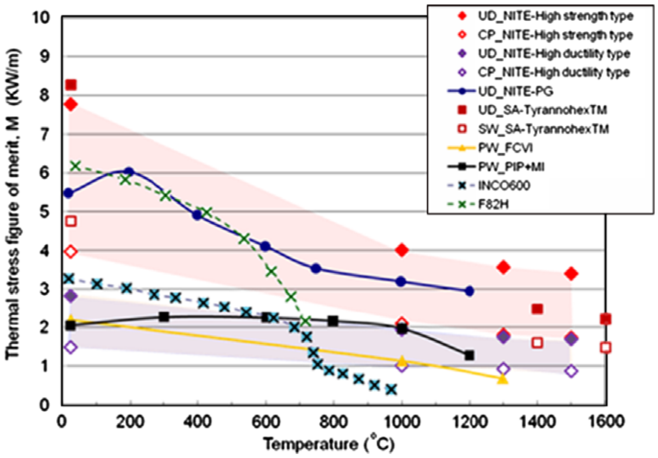

Fig. 6. Thermal stress tolerance of two kinds of NITE-SiC/SiC composites comparing with other high-temperature materials.

3.4. Thermal stress figure of merit

Fig. 6 shows the thermal stress figure of merit of metallic materials for high temperature applications, F82H steel and nickel-chromium alloy inconel 600 and advanced SiC/SiC composites including two kinds of prepared NITE-SiC/SiC composites. Metallic alloys have the relative high thermal figure of merit value from room temperature to 700 °C. Even for the conventional SiC/SiC composites fabricated by FCVI- and PIP+MI-process, however, the advantage became clear over 700 °C. The thermal stress figure of merit of high strength type showed the excellent value up to 1500 °C as well or better, compared with that of Tyranno-SA fiber-bonded ceramics (SA-Tyrannohex™), calculated from catalogue date.

4. Summary

The thermal stability of advanced SiC/SiC composites including two kinds of NITE-SiC/SiC composites in the active oxidation region was evaluated by high-temperature mechanical properties and microstructural evolution. Furthermore, thermal properties up to 1500 °C were investigated in Ar atmosphere. The results are as follows:

(1) Little matrix densification inter-fiber-tow caused a slight burnout of carbon interface, resulting in the severe degradation in strength.
(2) In NITE-composites, excess additional additives for matrix densification had possibility to form pores derived from the oxide segregations with the weight loss over 1300 °C. Higher-temperature fabricated composites as small as possible additional additives were able to enhance microstructural stability, resulting in the excellent retention of strength.
(3) The thermal conductivity of two kinds of NITE-SiC/SiC composites was much higher than that of CVI-SiC/SiC composites, which was able to satisfy the assume design value for fusion reactors.
(4) High strength type showed the excellent thermal stress figure of merit from room to high temperature.

Acknowledgements

This work was partly supported by supported by Fundamental R&D on Advanced Material system for (High Efficiency Environment-conscious) Very High-Temperature Gas-cooled Fast Reactor Core Structures, the program funded by Ministry of Education, Culture, Sports and Technology of Japan.

References

[1] R. Naslain, Compos. Sci. 64 (2004) 155.

[2] B. Riccardi, L. Giancarli, A. Hasegawa, Y. Katoh, A. Kohyama, R.H. Jones, L.L. Snead, J. Nucl. Mater. 329–333 (2004) 56.

[3] A. Kohyama, Mater. Trans. 46 (3) (2005) 1388.

[4] T. Nozawa, T. Hinoki, L.L. Snead, Y. Katoh, A. Kohyama, J. Nucl. Mater. 329–333 (1–3) (2004) 544.

[5] I.M. Low, Ceramic Matrix Composites-Microstructure, Properties and Applications, Woodhead Publishing, Abington, England, 2006.

[6] A. Kohyama, S.M. Dong, Y. Katoh, Ceram. Eng. Sci. Proc. 23 (3) (2002) 311.

[7] Y. Katoh, S.M. Dong, A. Kohyama, Fusion Eng. Des. 61&62 (2002) 723.

[8] S.M. Dong, Y. Katoh, A. Kohyama, J. Eur. Ceram. Soc. 23 (2003) 1223.

[9] K. Shimda, J.-S. park, T. Hinoki, A. Kohyma, Ceram. Eng. Sci. Proc. 27 (2) (2007) 207.

[10] K. Shimoda, J.-S. Park, T. Hinoki, A. Kohyama, Compos. Sci. 68 (1) (2008) 98.

[11] K. Shimoda, N. Eiza, J.-S. Park, T. Hinoki, A. Kohyama, Mater. Trans. 47 (4) (2006) 1204.

[12] L. Giancarli, H. Golfier, S. Nishio, R. Raffray, C. Wong, R. Yamada, Fusion Eng. Des. 61&62 (2002) 307.

[13] L. Giancarli, G. Aiello, A. Caso, A. Gasse, G. le Marois, Y. Poitevin, J.F. Salavy, J. Szczepanski, Fusion Eng. Des. 48 (2000) 509.